

## Optimal ray-tracing schemes in the mid-IR range through the main model shapes of rough and polished diamonds

© Y.S. Gulina<sup>1</sup>, R.A. Khmel'nitsky<sup>1,2</sup>, O.E. Kovalchuk<sup>1,3</sup>

<sup>1</sup> Lebedev Physical Institute, Russian Academy of Sciences,  
119991 Moscow, Russia

<sup>2</sup> Fryazino Branch, Kotel'nikov Institute of Radio Engineering and Electronics, Russian Academy of Sciences,  
141190 Fryazino, Moscow oblast, Russia

<sup>3</sup> Research and Development Geological Company Alrosa (PAO),  
678175 Mirny, Russia

e-mail: gulinays@lebedev.ru

Received November 11, 2022

Revised December 10, 2022

Accepted January 28, 2023

An analysis of ray-tracing schemes in the mid-IR range through the main model forms of rough and polished diamonds used for determining content of basic defects based on optical absorption measurements has been carried out. It is shown that in the traditional transmission measurement scheme only a small fraction of the radiation incident on the crystal is detected due to refraction and scattering in many crystals, leading to decreasing of the signal-to-noise ratio and to narrowing of the signal levels dynamic range. Practical recommendations are given and optimal variants of ray-tracing schemes through the most characteristic crystal shapes are proposed. This makes it possible to detect the maximum fraction of the radiation transmitted through the crystal, and to implement effective measurements of optical absorption in a wide dynamic range to determine the concentrations of basic defects with a high signal-to-noise ratio.

**Keywords:** Rough/faceted diamonds, optical active defects, optical transmission/absorption measurement, signal dynamic range, ray tracing.

DOI: 10.61011/EOS.2023.02.55793.1-23

### Introduction

Optically active defects in a diamond provide optical IR absorption (A-, B1-, B2-, C-, NVH defects) and UV visible absorption (A-, B1-, C defects and N2, N3 defects) [1–7]. Concentrational sensitivity in these two ranges is different. Each crystal has its own set of defects which defines its identity. Internal composition analysis of defects at all crystal handling stages enables efficient tracking by impurity/defect composition throughout the path beginning from the diamond mining to jewelry making [8].

In order to determine the composition and concentration of the main optically active defects in the diamond whose concentration is 1 ppm and higher, IR optical absorption spectroscopy is used [9,10]. The range from 400 cm<sup>-1</sup> to 5000 cm<sup>-1</sup>, where all necessary details are contained, may be divided into three subranges [11]. Single-phonon range from 400 cm<sup>-1</sup> to 1400 cm<sup>-1</sup> contains absorption bands of the main nitrogen defects for which there are calibration factors for optical absorption conversion into defect concentration [12]. Two-phonon range (1400 cm<sup>-1</sup> to 2665 cm<sup>-1</sup>) describes the intrinsic absorption of the diamond, three-phonon range (2665 cm<sup>-1</sup> to 4000 cm<sup>-1</sup>) also shows the intrinsic absorption and can additionally contain absorption bands of nitrogen/hydrogen and radiation defects [13,14]. Two-phonon intrinsic IR absorption may

be used as an internal optical path length standard of the crystal [15]. However, at a long optical path, the signal may be lower than the noise level as a result of strong attenuation. At high concentration of some defects (A-, B1-, B2-, C defects) in the single-phonon range, signal attenuation below the noise level may be also observed in the IR band. In this case, it is a good practice to use a measurement diagram with a minimum optical path length. On the other hand, to increase concentrational sensitivity for low-nitrogen diamonds, use a measurement diagram with a maximum optical path length and wide aperture.

For IR absorption measurements, the required concentrational sensitivity range is equal to 4 orders of magnitude: 1–10000 ppm [16,17]. To determine the composition and concentration of optically active defects in the diamond by means of optical absorption measurement, researchers generally use crystals or plates with at least two approximately parallel polished faces. However, this is rarely used for jewelry crystals — window repolishing is used only occasionally mainly to detect visible internal defects, for crystals with very rough surface or opaque coat. Most of diamond cuts are made such as to ensure the maximum possible light reflection. While for gemology purposes, the composition of the main defects shall be defined reliably in the characteristic volume of the uncut crystal which will be present in the diamond after cutting. This is usually

the central part of a crystal. However, spectrophotometers and IR spectrometers with traditional transmission measurement configuration record only a minor light fraction passing through many unafaced (in particular, rough and round) and fine-cut crystals — the main portion of light is reflected, diffracted and scattered at the crystal faces without penetrating into the receiver entrance aperture. The situation is aggravated by a high refraction index of the diamond and small crystal sizes. All these considerable, sometimes by two or more orders, reduces the signal level and, therefore, signal-to-noise ratio and results in reduction of the concentrational sensitivity range.

Thus, it is important to develop the best ray tracing diagram options in unafaced and nonparallelly faceted diamonds for efficient optical absorption measurement in the widest possible dynamic range with maximum signal-to-noise ratio.

## Ray tracing calculation diagram and crystal model shapes

Ray tracing through crystals of various shapes was simulated using Zemax software package. The simulation diagram established on the basis of „Bruker70v“ vacuum IR Fourier spectrometer is shown in Figure 1. The studied crystal is placed in the measuring orifice plane and exposed to IR radiation with a wavelength of  $\lambda = 10\ \mu\text{m}$  and beam diameter of  $D = 2\ \text{mm}$  by energy level  $1/e^2$ . The radiation that has passed through the specimen fall on a 6 cm Fourier spectrometer mirror located at 26 cm from the orifice plane. For the purpose of simulation, it is assumed that all radiation falling on the focusing mirror is collected by the radiation receiver.

The appearance of the majority of natural monocrystalline diamonds is limited by three main geometrical shapes: octahedron, cube and rhombic dodecahedron. However, only octahedral and cubic shapes constitute the true growth shapes of monocrystalline diamonds [2,18]. Very few diamonds approach the ideal octahedron, most of them are distorted. Irregular-shaped diamonds occur often and frequently constitute even a majority of diamonds at some deposits. In addition to the absence of well developed crystal faces, many diamonds are usually characterized by distinctly smooth and wavy surfaces. The study included simulation of radiation passage through several model shapes describing real natural crystals: 1. Regular octahedron — simulates smooth-face natural octahedral crystals. 2. Ball — simulates heavily dissolved round crystals. 3. —Round cut diamond.

## Results and discussion

### 1. Octahedron

When the ray beam goes through a homogenous octahedron, in addition to refraction, effects of reflection and re-

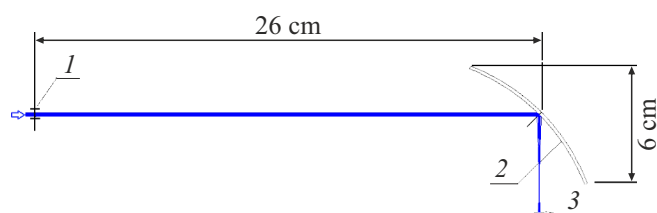


**Figure 1.** Ray tracing simulation diagram: 1 — measuring orifice, 2 — focusing mirror, 3 — radiation receiver.

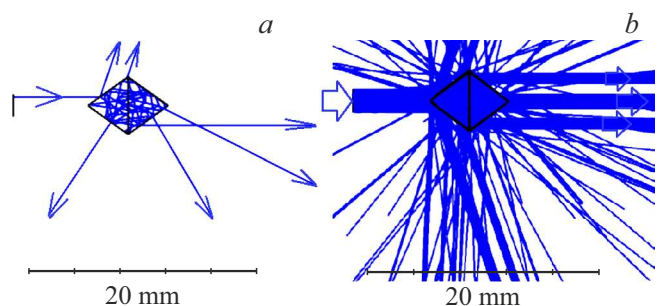


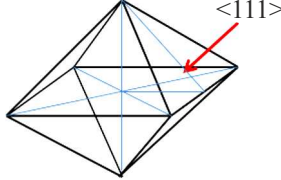
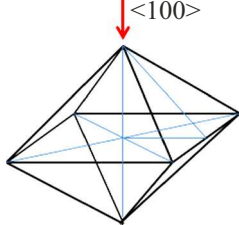
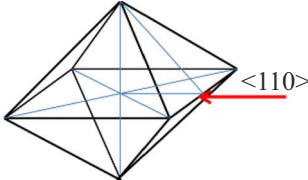
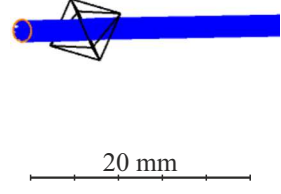
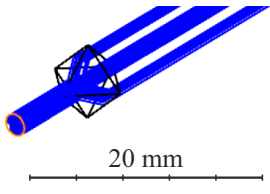
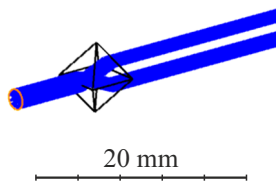
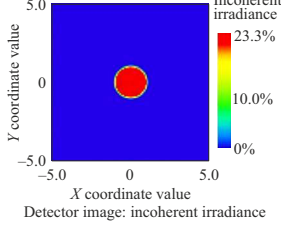
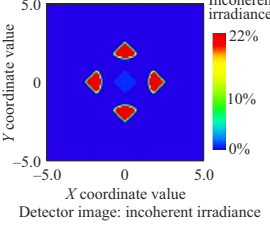
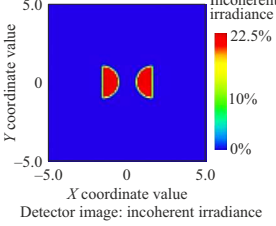
**Figure 2.** Single ray path (a) and wide ray beam path (b) through the octahedron including reflection and re-reflection effects.

reflection from smooth faces occur resulting in the reduction of energy fraction falling on the focusing mirror. These effects are demonstrated in Figure 2, a which shows ray path 1 through the octahedron with edge  $a = 5\ \text{mm}$ . On each face, in addition to the refracted component, a reflected component occurs resulting in many additional rays, and ambient illumination and power loss occur. Figure 2, b shows a wide ray beam path through the octahedron including reflection and re-reflection effects.

Since faces 111 in the octahedron are mutually parallel, we deal with the task of light passage through a set of plane parallel plates with a limited area at different light incidence angles. We have considered three orientation options of an octahedron with edge  $a$  against a light ray:  $\langle 111 \rangle$ ,  $\langle 100 \rangle$ ,  $\langle 110 \rangle$ . The main calculation results taking into account the diamond refraction index  $n = 2.38$  are summarized in a table. The diagrams of ray paths through the octahedron show only the rays that entered the receiver entrance aperture.

Analysis based on ray tracing has shown that the maximum signal level, when optical transmission of the octahedral diamond crystal is measured, is achieved in  $\langle 111 \rangle$  light incidence scheme with the radiation fraction, that has passed through the crystal and is recorded by the receiver, equal to about 70%. In addition,  $\langle 111 \rangle$  orientation is the most suitable for measurements because the crystal may be merely glued on or pressed to the orifice with its face  $\{111\}$ . For this a round orifice with the minimum diffraction may be used. The orifice shall be symmetrically inscribed into triangular face  $\{111\}$ . There is no light ray offset due to perpendicular incidence.

**Table 1.** The main results of ray beam tracing through the regular octahedron

Diagram	$\langle 111 \rangle$	$\langle 100 \rangle$	$\langle 110 \rangle$
of radiation incidence on the octahedron			
Ray beam path through the octahedron without taking into account the reflection and re-reflection effects			
Irradiance distribution in the mirror focusing plane; octahedron% entrance irradiance is assumed as 100%			
Radiation angle to the normal to the face $\{111\}$	$0^\circ$	$54.7^\circ$	$35.3^\circ$
Refraction angle on the face $\{111\}$ within the octahedron	$0^\circ$	$20^\circ$	$14^\circ$
Light passage aperture through the octahedron	$0.25a^2$	$0.5a^2$	$0.479a^2$
Optical path length within the octahedron	$0.816a$	$0.868a$	$0.841a$
Maximum light beam axis offset from the initial direction	0	$0.5a$	$0.305a$
Passage coefficient by the irradiance of the whole crystal	0.71	0.651	0.687

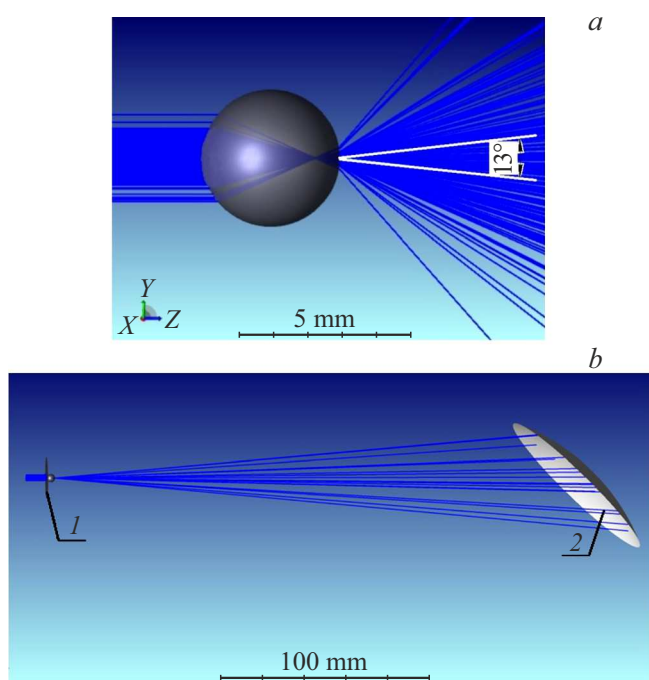


**Figure 3.** Diagram of ray path through a 4 mm (a) smooth ball without orifice (1), (b) with orifice. 2 — focusing mirror.

## 2. Ball

Ray path diagram for paraxial, plane parallel ray beam incidence on a smooth ball is shown in Figure 3,*a*. When the beam size is comparable with the spherical diamond size, due to high refraction index of the diamond, radiation passing through the sphere forms a widely diverging beam — the major light portion is re-reflected and scattered creating scattered radiation in the spectrophotometer, which is particularly undesired for UV and visible range measurements. To minimize the scattered and re-reflected radiation, it is a good practice to use an orifice whose size shall ensure the maximum illumination of the focusing mirror in order to achieve the maximum illumination in the image plane (Figure 3,*b*). The optimum orifice analysis carried out for 13° angular receiver aperture typical of Bruker 70v IR Fourier spectrometer are shown in Figure 4,*a*.

According to the analysis of radiation fraction falling on the receiver depending on the orifice size as shown in Figure 4,*a*, the orifice size shall satisfy  $d \leq 0.13D$ , while the radiation fraction falling on the receiver will be about 10%, and the scattered and re-reflected radiation will be vignettted. With a larger orifice, stray radiation is not fully intersected. Orifice size  $d = 0.13D$  is usually maximum 1 mm. In the visible and UV ranges, such size is acceptable from the point of view of scattered radiation reduction. And diffraction on the orifice is still low. In the average IR range (wavelength about 10 μm), diffraction on such small orifice will be apparent as the simulation shows. Moreover, scattered radiation almost does not interfere with the measurements in IR Fourier spectrometers. Therefore,

for IR range, we recommend to use a larger orifice, for example,  $d = 0.5D$  and even more provided that the crystal fully covers the orifice. Besides, this removes the high requirements for orifice installation accuracy illustrated in Figure 4,*b*, and, in case of crystal shapes different from the ideal ball, removes the need for the search of the best orifice position.

## 3. —Round cut diamond

In cut diamonds, optical transmission measurement is hindered because the cutting ensures maximum internal light reflection. Thus, when the beam is perpendicular to the pad, all radiation is reflected from the diamond faces and exits in reverse direction as shown in Figure 5,*a*. The analysis has shown that for a round-cut diamond, radiation entrance through the pavilion parallel to the pad is the best option. In this case, the light beam is refracted on the pavilion faces at the entrance, fully internally reflected from the pad edge and once more refracted on the pavilion edges at the exit (Figure 5,*b*). Due to the axial symmetry of cutting, light exits in the same direction as at the entrance. In this configuration, radiation passes through the material on the top of the diamond (crown area). This volume generally corresponds to the center of the initial crystal, from which the diamond is cut. Upper edge of the orifice shall be located in the girdle plane (as shown in Figure 5,*b*). According to the calculations, the best size of the round orifice is  $d = 0.14D_R$ , where  $D_R$  is the girdle diameter. In this case, the energy fraction falling into the receiver entrance orifice achieves 55%. Further increase in the orifice almost does not result in the signal increase due to addition of rays exposed to more than one reflections in the crystal and exiting in other directions, i.e. re-reflected and scattered radiation. It is natural that deviation from the best symmetrical position of the measuring orifice in relation to the diamond results in signal reduction (Figure 6).

The best orifice size  $d = 0.14D_R$  is usually maximum 1 mm. As in case with round crystals measured in IR range, we recommend to use a larger orifice, for example,  $d = 0.3D_R$ , and to place it above the position shown in Figure 5,*b* so that the orifice center is closer to the girdle plane. This also reduces the requirements for the orifice installation accuracy as shown in Figure 6.

## Conclusion

The investigations have shown that traditional optical transmission measurement in uncut and faceted diamonds is very inefficient in some cases due to heavy light refraction and scattering on the crystal. The best options are offered for diagrams of ray tracing through the main model shapes describing uncut and faceted diamonds implementing efficient optical absorption measurements in a wide dynamic range to determine concentrations of the main defects with high signal-to-noise ratio. It was shown

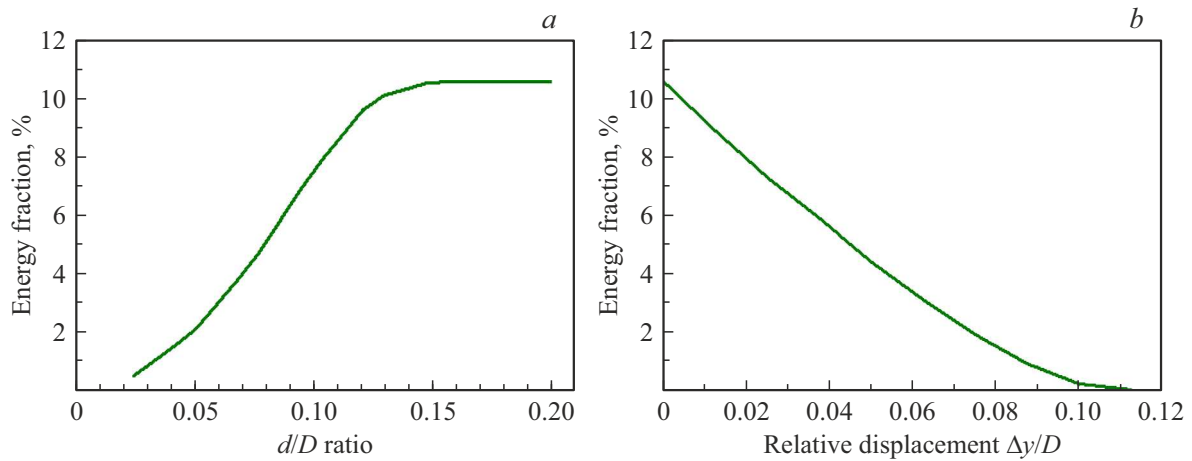


**Figure 4.** (a) Dependence of radiation fraction falling on the receiver on the ratio of orifice diameter  $d$  and ball diameter  $D$ . (b) Dependence of radiation fraction falling on the receiver on relative displacement  $\Delta y/D$  from the centerline of the ball with diameter  $D$ .

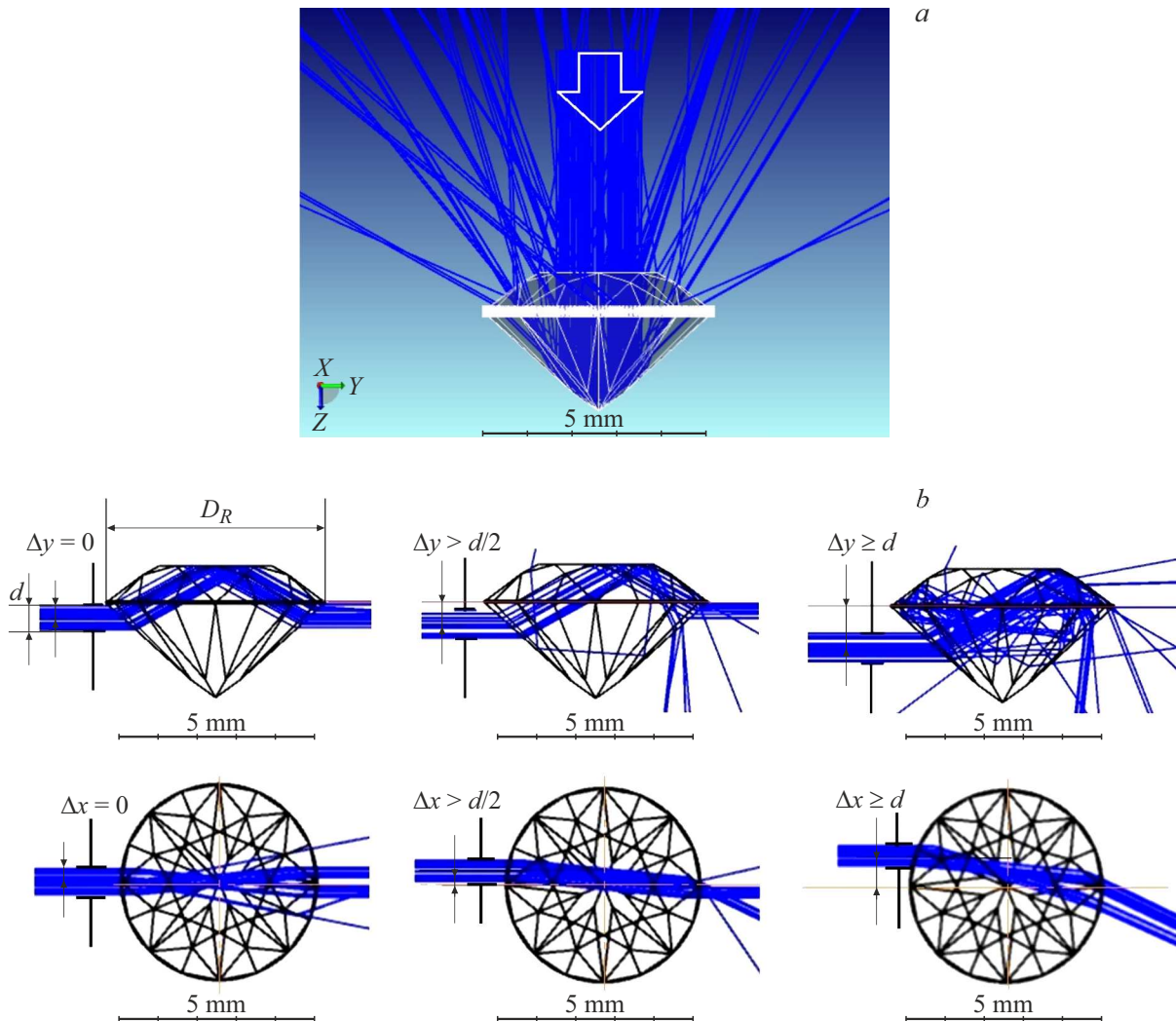


**Figure 5.** Diagrams of ray beam tracing through a round-cut diamond: (a) with normal beam incidence on the pad; (b) with beam introduction through the pavilion parallel to the pad with vertical displacement  $\Delta y$  and horizontal displacement  $\Delta x$  of beam axis.

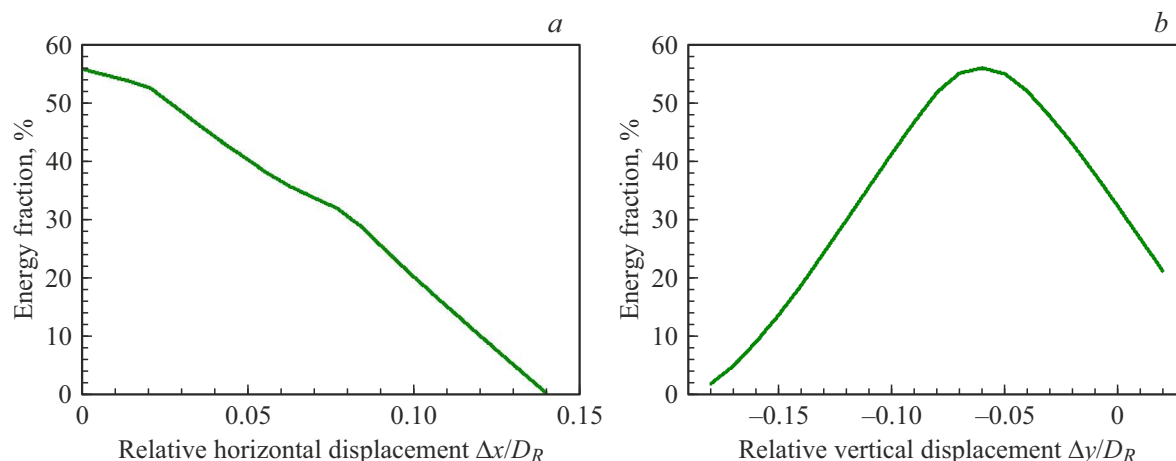


**Figure 6.** Dependence of radiation fraction recorded by the receiver with orifice size  $d = 0.14D_R$  on horizontal displacement  $\Delta x$  (a) and vertical displacement  $\Delta y$  (b) of ray beam axis from the centerline/girdle plane.

that the maximum signal level for octahedral diamonds during the optical transmission measurement is achieved in „111“ diagram of light incidence on the crystal, while the fraction of radiation recorded by the receiver is equal to about 70%. To minimize the influence of the scattered and re-reflected radiation during beam passage through the spherical diamond, use an orifice with size  $d < 0.13D$  with about 10.5% of the radiation falling on the receiver. In round-cut diamonds, the best measurement diagram is when the light is directed to the pavilion edges parallel to the girdle plane, while the best size of the round orifice is  $d = 0.14D_R$ . In this case, radiation fraction falling into the receiver entrance aperture achieves 55%.

### Funding

The authors are grateful to the Russian Science Foundation for the financial support of these research within project 21-79-30063.

### Conflict of interest

The authors declare that they have no conflict of interest.

### References

- [1] M.N.R. Ashfold, J.P. Goss, B.L. Green, P.W. May, M.E. Newton, C.V. Peaker. *Chem. Rev.*, **120** (12), 5745 (2020). doi: 10.1021/acs.chemrev.9b00518
- [2] R.A. Khmel'nitskii. *Introduction to Diamond Gemology* (Alrosa Technology, Moscow, 2021).
- [3] S.R. Boyd, I. Kiflawi, G.S. Woods. *Philos. Mag. B*, **69** (6), 1149 (1994). doi: 10.1080/01418639408240185
- [4] A.M. Zaitsev. *Optical Properties of Diamond: A Data Handbook* (Springer, Berlin/Heidelberg, Germany, 2013).
- [5] A.T. Collins. *Phys. B (Amsterdam)*, **185** (1-4), 284 (1993). doi: 10.1016/0921-4526(93)90250-A
- [6] H. Sumiya, S. Satoh. *Diamond Relat. Mater.*, **5** (11), 1359 (1996). doi: 10.1016/0925-9635(96)00559-6
- [7] S.I. Kudryashov, P.A. Danilov, N.A. Smirnov, A.O. Levchenko, M.S. Kovalev, Y.S. Gulina, O.E. Kovalchuk, A.A. Ionin. *Opt. Mater. Express*, **11** (8), 2505 (2021). doi: 10.1364/OME.427788
- [8] R. A. Khmel'nitsky, O.E. Kovalchuk, Y.S. Gulina, A.A. Nastulyavichus, G.Y. Kriulina, N.Y. Boldyrev, S.I. Kudryashov, A.O. Levchenko, V.S. Shiryayev. *Diamond Relat. Mater.*, **128**, 109278 (2022). doi: 10.1016/j.diamond.2022.109278
- [9] R.P. Mildren. *Opt. Eng. Diamond*, **1**, 1 (2013). doi: 10.1002/9783527648603.ch1
- [10] K.M. McNamara, B.E. Williams, K.K. Gleason, B.E. Scruggs. *J. Appl. Phys.*, **76** (4), 2466 (1994). doi: 10.1063/1.357598
- [11] F.V. Kaminsky, G.K. Khachatryan. *The Canadian Mineralogist*, **39** (6), 1733 (2001). doi: 10.2113/gscanmin.39.6.1733
- [12] S.D. Smith, J.R. Hardy. *Philos. Mag.*, **5** (60), 1311 (1960). doi: 10.1080/14786436008238345
- [13] J.R. Hardy, S.D. Smith. *Philos. Mag.*, **6** (69), 1163 (1961). doi: 10.1080/14786436108239677
- [14] C.A. Klein, T.M. Hartnett, C.J. Robinson. *Phys. Rev. B*, **45** (22), 12854 (1992). doi: 10.1103/PhysRevB.45.12854
- [15] D. Howell, C.J. O'Neill, K.J. Grant, W.L. Griffin, N.J. Pearson, S.Y. O'Reilly. *Diamond Relat. Mater.*, **29**, 29 (2012). doi: 10.1016/j.diamond.2012.06.003
- [16] Y. Zheng, C. Li, J. Liu, J. Wei, H. Ye. *Functional Diamond*, **1** (1), 63 (2022). doi: 10.1080/26941112.2021.1877021
- [17] M.I. Rakhmanova, A.Y. Komarovskikh, Y.N. Palyanov, A.A. Kalinin, O.P. Yuryeva V. A. Nadolniny. *Crystals*, **11** (4), 366 (2021). doi: 10.3390/cryst11040366
- [18] R. Tappert, M.C. Tappert. *Diamonds in Nature: A Guide to Rough Diamonds* (Springer Science & Business Media, 2011).

*Translated by E.Ilyinskaya*